THE JOURNAL OF BIOLOGICAL CHEMISTRY
Vol. 276, No. 16, Issue of April 20, pp. 13217–13225, 2001

Printed in U.S.A.

The TXP Motif in the Second Transmembrane Helix of CCR5

A STRUCTURAL DETERMINANT OF CHEMOKINE-INDUCED ACTIVATION*

Received for publication, December 26, 2000
Published, JBC Papers in Press, January 25, 2001, DOI 10.1074/jbc.M011670200

Cédric Govaerts‡§¶¶, Cédric Blanpain‡¶‖, Xavier Deupi, Sébastien Ballet‡, Juan A. Ballesteros‡‡, Shoshana J. Wodak§, Gilbert Vassart‡, Leonardo Pardo**, and Marc Parmentier‡§§**

*From ‡Institut de Recherche Interdisciplinaire en Biologie Humaine et Nucléaire, Université Libre de Bruxelles, Campus Erasme, 808 route de Lennik, B-1070 Bruxelles, Belgium, **Laboratori de Medicina Computacional, Unitat de Bioestadística, Facultat de Medicina, Universitat Autònoma de Barcelona, 08193 Bellaterra, Spain, §Service de Conformation des Macromolécules Biologiques, Université Libre de Bruxelles, CP 160/16, Avenue F. Roosevelt, 1050 Bruxelles, Belgium, and ‡‡Novasite Pharmaceuticals Inc., San Diego, California 92121*

CCR5 is a G-protein-coupled receptor activated by the chemokines RANTES (regulated on activation normal T cell expressed and secreted), macrophage inflammatory protein 1α and 1β, and monocyte chemotactic protein 2 and is the main co-receptor for the macrophage-tropic human immunodeficiency virus strains. We have identified a sequence motif (TXP) in the second transmembrane helix of chemokine receptors and investigated its role by theoretical and experimental approaches. Molecular dynamics simulations of model α-helices in a nonpolar environment were used to show that a TXP motif strongly bends these helices, due to the coordinated action of the proline, which kinks the helix, and of the threonine, which further accentuates this structural deformation. Site-directed mutagenesis of the corresponding Pro and Thr residues in CCR5 allowed us to probe the consequences of these structural findings in the context of the whole receptor. The P84A mutation leads to a decreased binding affinity for chemokines and nearly abolishes the functional response of the receptor. In contrast, mutation of Thr-82$^{2.56}$ into Val, Ala, Cys, or Ser does not affect chemokine binding. However, the functional response was found to depend strongly on the nature of the substituted side chain. The rank order of impairment of receptor activation is P84A > T82V > T82A > T82C > T82S. This ranking of impairment parallels the bending of the α-helix observed in the molecular simulation study.

Chemokine receptors are currently one of the most extensively studied subfamilies of G-protein-coupled receptors (GPCRs).[1] This is due to their key role in the immune response, where they act as attractors and stimulators of specific leukocyte populations (1), and their essential role in HIV infection. In particular, the chemokine receptor CCR5 is the main co-receptor for macrophage-tropic HIV-1 strains, which are responsible for disease transmission and predominate during the asymptomatic phase of the disease (2, 3). It hence appears as one of the crucial targets for developing new therapeutic strategies against HIV.

CCR5 is activated by the chemokines RANTES, MIP-1α, MIP-1β, and MCP-2 and binds a natural chemokine antagonist, MCP-3 (4). Chemokines are small globular proteins, 60–100 residues long, comprising a well structured domain, and a flexible NH_2 terminus, with a Cys-Cys or Cys-*X*-Cys motif (where *X* represents a variable residue) marking the limit between the two parts (1).

The mechanisms by which chemokines bind their receptors and induce activation are currently unclear. Mutagenesis studies of chemokines suggest that a major role in binding is played by receptor interactions with their compact domain, while the flexible NH_2 terminus is required mainly for receptor activation (5, 6). NH_2-terminally truncated chemokines usually bind their receptors with wild type affinities but elicit a severely impaired functional response (6, 7).

On the receptor side, several studies have shown that its extracellular domains play an essential role in chemokine binding (8, 9). In particular, the NH_2-terminal domain of the receptor was shown to be mandatory for chemokine binding, with several charged and aromatic residues playing a crucial role (10, 11). On the other hand, some of us have shown that most of the ligand specificity is encoded in the second extracellular loop of CCR5 (12).

Clearly belonging to the rhodopsin-like family of GPCRs, chemokine receptors share all of the highly conserved sequence motifs characteristic of this family. The overwhelming majority of these sequence motifs are located in the transmembrane region, suggesting the conservation of a common fold for this region throughout the entire rhodopsin-like family. The existence of a conserved fold may in turn imply similar mechanisms

* This work was supported by the Actions de Recherche Concertées of the Communauté Française de Belgique, the French Agence Nationale de Recherche sur le SIDA, the Center de Recherche Inter-universitaire en Vaccinologie, the Belgian program on Interuniversity Poles of Attraction initiated by the Belgian State, Prime Minister's Office, Science Policy Programming, BIOMED and BIOTECH programs of the European Community Grants BIO4-CT98-0543 and BMH4-CT98-2343, the Fonds de la Recherche Scientifique Médicale of Belgium, Télévie, and the Fondation Médicale Reine Elisabeth (to M. P). This work was also supported in part by Comisión Interministerial de Ciencia y Tecnología, Spain Grant SAF99-073, Fundació La Marató TV3 Grant 0014/97, and Improving Human Potential of the European Community Grant HPRI-CT-1999-00071. Computer facilities were provided by the Center de Computació i Comunicacions de Catalunya. The costs of publication of this article were defrayed in part by the payment of page charges. This article must therefore be hereby marked "*advertisement*" in accordance with 18 U.S.C. Section 1734 solely to indicate this fact.

¶ These two authors contributed equally to this work.
‖ Aspirant of the Belgian Fonds National de la Recherche Scientifique.
§§ To whom correspondence should be addressed. Tel.: 32 2 555 41 71; Fax: 32 2 555 46 55; E-mail: mparment@ulb.ac.be.
¶¶ Fellow of the Fonds pour la Formation à la Recherche dans l'Industrie et dans l'Agriculture.

[1] The abbreviations used are: GPCR, G-protein-coupled receptor; HIV, human immunodeficiency virus; TM, transmembrane helix; PK, proline kink; MD, molecular dynamics; MIP, macrophage inflammatory protein; MCP, monocyte chemotactic protein; WT, wild type; RANTES, regulated on activation normal T cell expressed and secreted.

in receptor activation involving the membrane-embedded portion of the proteins.

A detailed atomic model representing this common fold has at long last become available with the recent determination of the high resolution x-ray structure of bovine rhodopsin (13). This structure confirms the well documented seven-transmembrane α-helix bundle topology, proposed on the basis of lower resolution structural studies (14). It furthermore provides a detailed atomic picture of the interactions between the transmembrane helices, particularly those involving the conserved GPCR sequence motifs.

It has been established that for many receptors, which are activated by small ligands like neurotransmitters, agonist binding and subsequent triggering of activation involves a water-accessible pocket centrally located within the transmembrane helix bundle. This pocket corresponds roughly to the retinal binding site in rhodopsin (15–17). The strong similarity of the transmembrane regions of chemokine receptors to those of other rhodopsin-like GPCRs suggests that these proteins undergo ligand-induced activation processes, involving analogous conformational changes. Some of these changes have been monitored for various GPCRs, using different techniques (for a review, see Ref. 17). In particular, transmembrane helix 6 (TM6) was reported to rotate its cytosolic end away from TM3 in several receptors (18–24).

This crucial rigid body motion of a part of TM6 is thought to be enabled by the presence of a highly conserved proline in the middle of the helix (25), which introduces a local break in the helix structure. Such a break, denoted a proline kink (PK), is likely to impart the backbone flexibility (16, 26–28) required for the conformational change associated with the activation process. Mutations of the conserved Pro in TM6 in several receptors were indeed shown to produce phenotypes ranging from severely impaired expression of the receptor (29) to reduced functional coupling (30) or even constitutive activation (31). Mutations of conserved prolines in other helices, notably TM5 (32) and TM7 (33, 34), were also found to cause significant perturbations. For instance, proline mutations in the conserved NP*XX*Y motif in TM7 often produce particularly strong phenotypes, including impaired activity (33, 35, 36).

However, although some of the structural rearrangements associated with activation are likely to be conserved throughout the rhodopsin-like receptor family, the extraordinary diversity of ligand types, ranging from small size neurotransmitters to large glycoprotein hormones (17), suggests that receptor subfamilies have presumably evolved specific binding modes with activation mechanisms probably requiring somewhat different structural adaptations.

This study investigates such subfamily-specific properties in the chemokine receptors. All chemokine receptors are shown here to share a proline in TM2. Analysis of their aligned sequences also reveals the presence of a conserved threonine residue 2 positions upstream of this Pro forming the T*X*P motif. Considering that threonine residues have been observed to induce small distortions in α-helices (37, 38), we hypothesize here that the conjunction of these two conserved and structurally relevant residues in chemokine receptors might constitute a key motif required for proper receptor function. The influence of Thr in Pro-containing helices had been identified earlier for other integral membrane proteins (39).

This hypothesis is investigated using an approach, which combines theoretical and experimental procedures. The theoretical procedures are aimed at characterizing the effect of the T*X*P motif on the intrinsic conformational properties of the transmembrane helix and on its putative interactions with other helices in the bundle. To this end, we have performed molecular dynamics (MD) simulations of an isolated polyalanine helix comprising a T*X*P motif and several variants thereof in which the Thr residue is replaced by other side chains, Ser, Cys, Val, and Ala, respectively. In addition, using the recently determined three-dimensional structure of rhodopsin as a template, the structural role of this motif in the context of the seven-helix bundle is assessed. This allows us to formulate hypotheses on how the conformational states of the T*X*P motif-containing helix might act to produce structural changes in the helix bundle.

The experimental procedures involve site-directed mutagenesis, in which the Thr of the T*X*P motif of TM2 in CCR5 is replaced by the same side chains as in the simulation analysis and where Ala is substituted for the Pro in order to abrogate the PK. The different CCR5 mutants are then tested in order to determine their ligand binding and activation properties.

Our results reveal a significant correspondence between the modulating effect on the Pro kink angle and helix conformational flexibility by Thr *versus* other residues in the T*X*P motif and the activation properties measured experimentally for the corresponding mutants in CCR5. The implications of these findings for chemokine-receptor interactions and chemokine-induced activation are discussed.

EXPERIMENTAL PROCEDURES

Numbering Scheme of GPCRs—In this work, we use a general numbering scheme to identify residues in the transmembrane segments of different receptors (28). Each residue is numbered according to the helix (helix 1 through 7) in which it is located and according to the position relative to the most conserved residue in that helix, arbitrarily assigned to 50. For instance, Pro-*2.58* is the proline in the transmembrane helix 2 (TM2), 8 residues following the highly conserved aspartic acid Asp-*2.50*.

*Survey of Helices Containing a T*X*P Motif in Known Protein Structures*—Since stable structural motifs are likely to recur in proteins of known structures (40), we also surveyed the recent release of the Protein Data Bank (Research Collaboratory for Structural Bioinformatics, Rutgers University, New Brunswick, NJ) for α-helical segments featuring a T*X*P, S*X*P, or C*X*P motif with no other Thr, Ser, or Cys within the PK and no other Pro anywhere in the segment. Since measuring the bending angle requires at least one helical turn prior to the PK and a helical turn following it, we selected helical segments of at least 12 residues. We performed our search in a nonredundant set of protein structures with resolutions of 3 Å or better, identifying 16 helical segments (Protein Data Bank numbers 1AR1, 1B7E, 1B94, 1BDB, 1BPO, 1FCB, 1FIY, 1FVK, 1OCC, 1PJC, 1REQ, 1RVE, 1TCO, 1VHB, 2AK3, and 2GST). Detailed analysis of the corresponding structures showed that most of these helices are exposed to solvent, with water molecules often interacting with the backbone at the level of the PK. Since such interactions are not likely to occur in a membrane-embedded helix, structures displaying these interactions were rejected, finally yielding only seven structures (see Table I). The bending angle of these structures is defined as the angle between the axes computed as the least square lines through the backbone atoms (N, C_α, C) of the α-helical part before and after the Pro kink (using the InsightII software, MSI, San Diego).

Molecular Dynamics Simulations of Transmembrane Helices—To study the conformational properties of an α-helix containing a T*X*P motif, we performed molecular dynamics simulations of the model peptides Ace-Ala_{11}-*XXX*-Ala_{11}-NMe, where *XXX* is either AAP, TAP, SAP, CAP, or VAP. These 25-residue peptides were built in the standard α-helical conformation (ϕ, ψ = 58°, −47°).

In a hydrophobic environment, the side chains of Ser, Thr, and Cys are most likely to form hydrogen bonds with other polar groups of the protein or of the ligand whenever present. Surveys of known protein structures (41, 42) show that in α-helices, these side chains hydrogen-bond primarily the carbonyl group in the preceding turn of the helix (residue i-4 or i-3).

For Thr and Ser, such bonds can form only in the $g+$ or $g-$ side chain conformations, whereas for Cys, they can be formed only in the $g+$ conformation. The $g-$ conformation of Cys is energetically unfavorable because of the steric clash between the S_γ atom and the carbonyl oxygen of residue i-3 (42). For these side chains, the t cannot form such hydrogen bonds as it points the OH group away from the backbone. The model

peptides were hence built with the Thr and Ser side chains in either $g+$ or $g-$ and with the Cys side chain in $g+$. The hydrophobic Val side chain was built in the t conformation.

Starting structures were placed in a rectangular box ($59 \times 37 \times 38$ Å) containing methane molecules at a density approaching half that of hydrocarbons in lipid bilayer, in order to mimic the plasma membrane environment. The peptide-methane systems were subjected to 500 iterations of energy minimization and then heated to 300 K in 15 ps. This was followed by an equilibration period (15–500 ps) and a production run (500–1500 ps). The simulations were carried out at constant volume and constant temperature (300 K), with the latter maintained through coupling to a heat bath. The particle mesh Ewald method was employed to compute electrostatic interactions (43). Structures were collected for analysis every 10 ps during the last 1000 ps of simulation. The molecular dynamics simulations were run with the Sander module of AMBER5 (44), using an all atom force field (45), the SHAKE bond constraints on all bonds, and a 2-fs integration time step.

Bending of the Pro containing peptides was measured as described above using backbone atoms of helical segments comprising residues 2–11 (before the Pro) and 16–24 (after the Pro). One-way analysis of the variance plus *a posteriori* one-sided Dunnett's t tests were performed to determine if the bend angles of the helices containing the TAP, SAP, CAP, and VAP motifs are greater than the bend angle of the helix containing the AAP motif, taken as reference. To choose representative structures for each trajectory, the structures saved during the production run were clustered on the basis of their relative backbone root mean square deviation using the NMRCLUST program (46) with a cut-off of 3 Å.

CCR5 Mutants—Plasmids encoding the CCR5 mutants studied here were constructed by site-directed mutagenesis using the QuickChange method (Stratagene). Following sequencing of the constructs, the mutated coding sequences were subcloned into the bicistronic expression vector pEFIN3 as previously described for generation of stable cell lines (12). All constructs were verified by sequencing prior to transfection.

Expression of Mutant Receptors in CHO-K1 Cells—CHO-K1 cells were cultured in Ham's F-12 medium supplemented with 10% fetal calf serum (Life Technologies, Inc.), 100 units/ml penicillin, and 100 μg/ml streptomycin (Life Technologies). Constructs encoding wild type or mutant CCR5 in the pEFIN3 bicistronic vector were transfected using Fugene 6 (Roche Molecular Biochemicals) in a CHO-K1 cell line expressing an apoaequorin variant targeted to mitochondria (47). Selection of transfected cells was made for 14 days with 400 μg/ml G418 (Life Technologies) and 250 μg/ml zeocin (Invitrogen; for maintenance of the apoaequorin-encoding plasmid), and the population of mixed cell clones expressing wild type or mutant receptors was used for binding and functional studies. Cell surface expression of the receptor variants was measured by flow cytometry using monoclonal antibodies recognizing different CCR5 epitopes; 2D7 (phycoerythrin-conjugated; Pharmingen), MC-1, MC-4, MC-5, and MC-6 (kindly provided by Mathias Mack, Medizische Poliklinik, Ludwig-Maximilians, University of Munich, Munich, Germany) were detected by anti-mouse IgG phycoerythrin-coupled secondary antibody (Sigma).

^{125}I-RANTES Binding Assays—CHO-K1 cells expressing wild type or mutant CCR5 were collected from plates with Ca^{2+}- and Mg^{2+}-free phosphate-buffered saline supplemented with 5 mM EDTA, gently pelleted for 2 min at $1000 \times g$, and resuspended in binding buffer (50 mM Hepes, pH 7.4, 1 mM $CaCl_2$, 5 mM $MgCl_2$, 0.5% bovine serum albumin). Competition binding assays were performed in Minisorb tubes (Nunc) with 40,000 cells in a final volume of 0.1 ml. The mixture contained 0.05 nM ^{125}I-RANTES (2000 Ci/mmol; Amersham Pharmacia Biotech) as tracer and variable concentrations of competitors (R & D Systems). Total binding was measured in the absence of competitor, and nonspecific binding was measured with a 100-fold excess of unlabeled ligand. Samples were incubated for 90 min at 27 °C, and then bound tracer was separated by filtration through GF/B filters presoaked in 0.5% polyethylenimine (Sigma) for ^{125}I-RANTES. Filters were counted in a β-scintillation counter. Binding parameters were determined with the Prism software (GraphPad Software) using nonlinear regression applied to a one-site competition model.

Functional Assays—Functional response to chemokines was analyzed by measuring the luminescence of aequorin as described (48, 49). Cells were collected from plates with Ca^{2+}- and Mg^{2+}-free Dulbecco's modified Eagle's medium supplemented with 5 mM EDTA. They were then pelleted for 2 min at $1000 \times g$, resuspended in Dulbecco's modified Eagle's medium at a density of 5×10^6 cells/ml, and incubated for 2 h in the dark in the presence of 5 μM coelenterazine H (Molecular Probes, Inc., Eugene, OR). Cells were diluted 5-fold before use. Agonists in a volume of 50 μl of Dulbecco's modified Eagle's medium were added to 50 μl of cell suspension (50,000 cells), and luminescence was measured for 30 s in a Berthold luminometer.

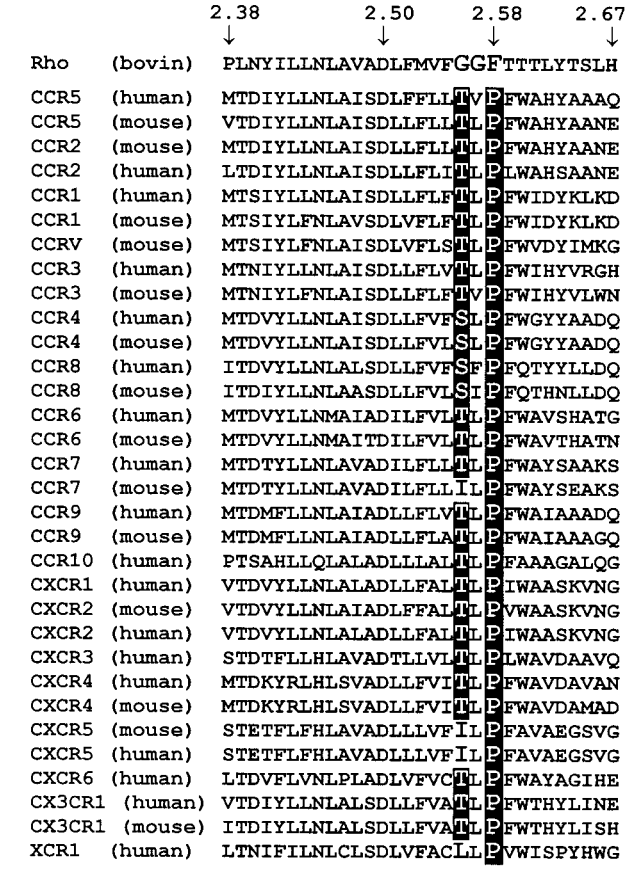

FIG. 1. **Alignment of TM2 sequences from chemokine receptors and bovine rhodopsin.** For the sake of clarity, only human and murine sequences are shown. The generalized numbering scheme (see "Experimental Procedures") is used to label the alignment. The T*X*P (or S*X*P) motif is indicated in *boldface characters*, and its conserved residues are *highlighted*. The sequence of TM2 of bovine rhodopsin is also aligned, showing the high homology between CCR5 and bovine rhodopsin in the cytosolic part of TM2, up to the T*X*P motif. Note that we make the assumption that, in chemokine receptors, TM2 extends to position *2.67* (included). This is based on the observation that TM2 extends to this residue in the three-dimensional structure of rhodopsin (13) and on the suggestion that position *2.67* terminates TM2 in the dopamine D2 receptor, on the basis of the substituted cysteine accessibility method (59).

RESULTS

A Conserved TXP Motif in TM2 of Chemokine Receptors—Multiple sequence alignments of the second transmembrane helix of 55 mammalian chemokine receptors were performed. Fig. 1 shows alignment of the human and mouse sequences, together with TM2 of bovine rhodopsin. Inspection of the aligned sequences reveals a highly conserved T*X*P sequence motif in TM2, where *X* represents a variable hydrophobic residue. Pro, at position $84^{2.58}$ (84 is the residue number in the CCR5 sequence, and *2.58* is the corresponding number in the general numbering scheme), is completely conserved across all chemokine receptors. The Thr residue is also highly conserved, present in 47 sequences out of 55, while Ser is found in four receptors. The last four receptors have an Ile or Leu in position *2.56*.

A survey of the 1200 rhodopsin-like GPCRs present in the G-protein Coupled Receptors Database (50) reveals that this motif is also found at the equivalent position in the sequences of about 50 non-chemokine receptors, comprising essentially peptidergic, such as angiotensin and opioid, receptors.

TABLE I
Bending angles for TXP motifs found in the Protein Data Bank (PDB)

Two segments are taken from the structure of cytochrome *c* oxidase (1AR1), which is a membrane protein. The other proteins are hemoglobin (1VHB), a phosphoenolpyruvate carboxylase (1FIY), a transposase inhibitor (1B7E), an endonuclease (1RVE), and the clathrin heavy chain (1BPO).

PDB no.	Motif	Helical segment	Position of the Pro	Bending angle
				degrees
1VHB	TVP	A7→A20	A15	28
1FIY	TDP	823→856	838	44
1B7E	TLP	349→379	373	49
1RVE	SRP	B37→B59	B50	26
1AR1	SLP	A219→A248	A236	35
1AR1	SLP	B85→B103	B98	29
1BPO	CRP	428→442	438	41

TABLE II
Bending angles measured in the different simulations

Average and S.D. of the bending angle obtained during the MD simulations are shown. Each value is obtained over a sample of 100 structures equally distant during the MD run (see "Experimental Procedures"). One-way analysis of variance plus *a posteriori* one-sided Dunnett's *t* tests were used to determine whether the bending angles of the different motifs are significantly larger than that of the control AAP. Asterisks denote statistically significant deviation from the AAP control ($p < 0.001$).

	Bending angle	S.D. value
	degrees	
AAP	19.9	7.3
TAP *g*+	28.4*	7.1
TAP *g*−	26.6*	7.8
SAP *g*+	30.1*	11.9
SAP *g*−	35.0*	10.0
CAP *g*+	31.3*	10.8
VAP	21.0	5.5

Fig. 1 also shows that the primary structure of bovine rhodopsin TM2 is highly similar to that of chemokine receptors from its NH_2 terminus (cytosolic border) to the T*X*P motif but strongly diverges between the T*X*P motif and its COOH terminus (beginning of ECL1). This suggests a structural and functional conservation in the cytosolic half of this transmembrane segment.

Influence of the TXP Motif on the Conformation of a Transmembrane Helix—To assess the influence of the T*X*P motif on the conformation of a transmembrane helix 2, complementary approaches were used. A first approach consisted in surveying known protein structures in the Protein Data Bank for α-helices containing either a T*X*P, S*X*P, or C*X*P motif, using the criteria specified under "Experimental Procedures." This resulted in identifying only seven structures, all of which displayed a strong bend, with angles ranging from 25 to almost 50° as shown in Table I. It is noteworthy that the reported average bend angle of α-helices containing Pro is about 25° (26). The helices identified here thus seem to be as strongly bent as, if not more strongly bent than, the average PK, but the very small number of observations precludes drawing a reliable conclusion.

A second approach was therefore undertaken. This involved performing molecular dynamics simulations on polyalanine helices, 25 residues long, embedded in a nonpolar solvent, and containing the AAP, TAP, SAP, CAP, and VAP motifs, respectively, in their midst. Table II lists the average helix kink angles in conformations along the MD trajectories. Representative structures from the different trajectories are displayed in Fig. 2, *A* and *B*.

We find that the presence of a single proline (AAP) or of the VAP motif produces helix bend angles of about 20°. For the simulation of the AAP containing peptide, our results agree with those of earlier simulation studies on Pro-containing polyalanine (51).

Significantly larger bending angles (27–35°) are observed when Thr, Ser, or Cys is introduced 2 positions before the Pro. Detailed analysis of the conformations in the trajectories show, as expected, that the side chain hydroxyl (or SH) groups of these residues form hydrogen bonds with the carbonyl group of residue i-4, in a significant proportion of the conformations (85–100%). Such hydrogen bonds are formed with Thr in the *g*+ or *g*− conformations, Ser in *g*+, and Cys in *g*+.

On the other hand, Ser in *g*− achieves and maintains hydrogen bonding with the carbonyl of residue i-3 position. This seemingly minor alteration in the hydrogen bonding pattern appears, however, to induce a dramatic modification in the conformation of the helix, as illustrated in Fig. 2*B*. Not only is the helix kink angle increased significantly, but the COOH-terminal moiety of the helix points to a completely different direction in space.

The results of our simulation analysis hence suggest that in a nonpolar environment, the nature of the residue located at position i-2 relative to the proline modulates the magnitude and direction of the PK through the formation of a hydrogen bond between the side chain and the backbone carbonyl group at position i-3 or i-4. In particular, the presence of Thr, Ser, and Cys side chains at position i-2 relative to the Pro increases the average helix bend angle by about 10°, whereas that of Val does not.

Accommodating a Kinked TM2 Helix in the Receptor Three-dimensional Structure—To obtain a rough idea on the possible consequences that the presence of T*X*P motif might have on the structure of the receptor, and more particularly on the TM region, we performed a molecular modeling exercise using the recently determined three-dimensional structure of bovine rhodopsin as the template. As shown in the alignment (Fig. 1), the sequence of TM2 is strongly conserved (~50% sequence identity) between chemokine receptors and rhodopsin between the cytosolic border and the T*X*P motif. This leaves no ambiguity in aligning the rhodopsin and CCR5 sequences in this region and allowed us to readily position representative structures from the simulations of the AAP and TAP containing model peptides into the TM bundle of rhodopsin. In particular, the backbone atoms of the two helical turns preceding the PK in our model peptides were superimposed on those of the two turns preceding the equivalent residue (in CCR5, the PK starts at *2.54*, four residues before Pro-*2.58*) in rhodopsin, respecting the correspondence of the sequence alignment. Interestingly, rhodopsin has two successive glycines in positions *2.56* and *2.57* (with a Phe and not a Pro at *2.58*, forming a GGF motif). Most probably as a result of the conjunction of these two flexible residues, its TM2 is strongly distorted, so that its extracellular part leans toward TM1.

Fig. 2 (*C* and *D*) shows the result of superimposing the representative structures from the TAP *g*+ (*red*) and AAP (*yellow*) simulations on TM2 of rhodopsin. Strikingly, the kink induced by Pro-*2.58* in AAP (*yellow*) orients the extracellular moiety of TM2 toward TM3 and away from TM1 (Fig. 2*C*). The presence of Thr in TAP, which, as shown above, increases the helix bend angle by about 10°, causes the extracellular side of TM2 to lean even more toward TM3 and slightly toward the center of the bundle (Fig. 2*D*). The differences in the amino acid sequences of the TM2 in the opsin (GGF) *versus* the chemokine (T*X*P) families may thus be related to structural differences in this region. In particular, in the chemokine receptors, the extracellular sides of TM2 and TM3 would come into close con-

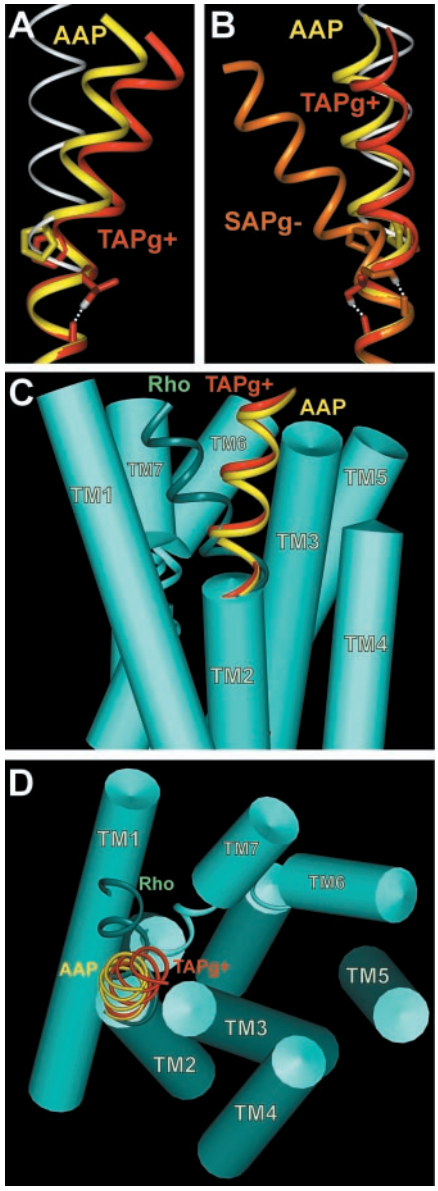

FIG. 2. **Effect of AAP and TAP *g*+ motif on the conformation of α-helices.** *A*, representative structures for AAP (*yellow*), TAP *g*+ (*red*), and an ideal α-helix (*white*). Backbones are represented as *ribbons*, and side chains of Pro and Thr are shown as *solid sticks* (with polar hydrogen in *white*) as well as the hydrogen bonding carbonyl, 4 residues before the Thr. Hydrogen bonds are indicated by *dotted white lines*. *B*, representative structures for AAP, TAP *g*+, SAP *g*− (orange), and an ideal α-helix. This view is rotated by 90° along the helical axis relative to *A*. In the *g*− rotamer, the Ser hydrogen bonds with carbonyl situated 3 residues upstream, which induces clearly a different orientation of the PK. *C*, the representative structure of the AAP (*yellow ribbon*) and TAP *g*+ (*red ribbon*) motifs are positioned in the rhodopsin template, respecting the homology between CCR5 and rhodopsin. The two representative helices were superimposed on the cytoplasmic end of TM2 in the rhodopsin structure (Protein Data Bank number 1F88), using backbone atoms up to position *2.54*. Rhodopsin (*turquoise*) helices are shown as *cylinders*, except for the extracellular part of TM2, which is shown as a *ribbon*. This panel is viewed from the side of the protein. *D*, same representation as in *C* but viewed from the extracellular side. The influence of the Thr on the PK is clearly visible, as it bends the helix inside the bundle.

tact. It is noteworthy that chemokine receptors have a cluster of aromatic residues at the extracellular end of TM2 and TM3. In other GPCRs, helix-helix interactions mediated by aromatic clusters are believed to play a role in ligand-induced receptor activation (52).

Effects of Mutations in the Conserved TXP Motif on CCR5 Expression and Function—To investigate the possible role of the TXP motif in CCR5 expression and function, several mutants were generated in the corresponding positions. Mutant P84$^{2.58}$A was built in order to completely eliminate the PK, while mutants T82$^{2.56}$S, T82$^{2.56}$C, T82$^{2.56}$V, and T82$^{2.56}$A were aimed at investigating the kink modulation effects produced by the same residues as those studied in the model peptide MD simulations.

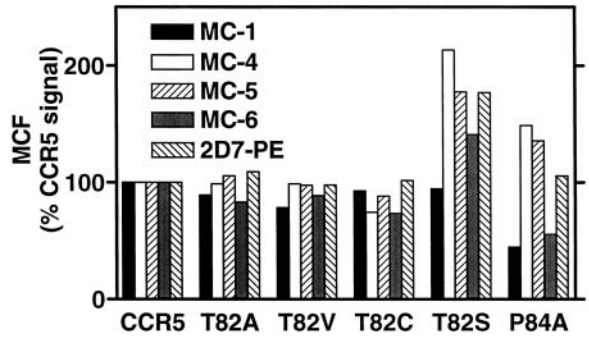

FIG. 3. **Level of expression of the receptors.** Cell surface expression of WT CCR5 and the different mutants was measured by fluorescence-activated cell sorting using five different monoclonal antibodies. The data are representative of three different experiments. The 2D7 antibody recognizes a conformational epitope centered on ECL2. We have recently identified the epitopes of the other antibodies tested here (C. Blanpain, M. Mack, J.-M. Vanderwinden, V. Wittamer, E. Le Poul, G. Vassart, and M. Parmentier, manuscript in preparation); MC-1 and MC-6 recognize multidomain conformational epitopes, while MC-4 targets a conformational NH_2-terminal epitope and MC-5 a linear epitope also located in the amino-terminal domain of CCR5. Values represent mean cell fluorescence normalized by the value obtained for CCR5 (100%) separately for each antibody.

Cell Surface Expression of the CCR5 Mutants—Cell surface expression of the CCR5 mutants was measured by fluorescence-activated cell sorting analysis using a set of monoclonal antibodies, recognizing various epitopes of the receptor, ranging from well defined linear epitopes in the NH_2-terminal domain (MC-5) to complex conformational epitopes spanning multiple domains (MC-6). As shown in Fig. 3, all mutants were properly expressed at the cell surface, as compared with the WT receptor. With the exception of P84A, the mutant receptors were recognized as similar levels by all monoclonals, suggesting that the mutations did not alter significantly the folding of the extracellular domain.

The pattern observed for the P84A mutant seems to indicate a deeper conformational modification for this mutant, which could in turn cause the alteration of the extracellular domain conformation and eventually affect conformational epitopes. Nevertheless, the antibodies recognizing the amino-terminal part of the receptor did detect the P84A mutant at the cell surface at levels similar to those observed for WT CCR5.

Chemokine Binding Properties of WT CCR5 and Mutant Receptors—The ability of the different CCR5 mutants to bind the four high affinity CCR5 agonists, the chemokines RANTES, MIP-1α, MIP-1β, and MCP-2, was tested by competition binding assays, using ^{125}I-RANTES as tracer. Fig. 4 shows the competition curves for the various constructs.

As shown earlier, RANTES appears as the strongest ligand for WT CCR5 (4), with an IC_{50} of 0.28 nM (Table III). The IC_{50} values for MIP-1α (3.7 nM), MIP-1β (1.3 nM), and MCP-2 (2.4 nM) are shifted to slightly higher values as compared with those obtained previously with ^{125}I-MIP-1β as tracer, but the order of potencies is conserved (Table III). Changes in apparent affinities as a function of the tracer used have been observed previously for chemokine and other receptors (9).

P84A is able to bind RANTES with WT affinity (IC_{50} = 0.25 nM), while MIP-1β and MCP-2 show significantly decreased

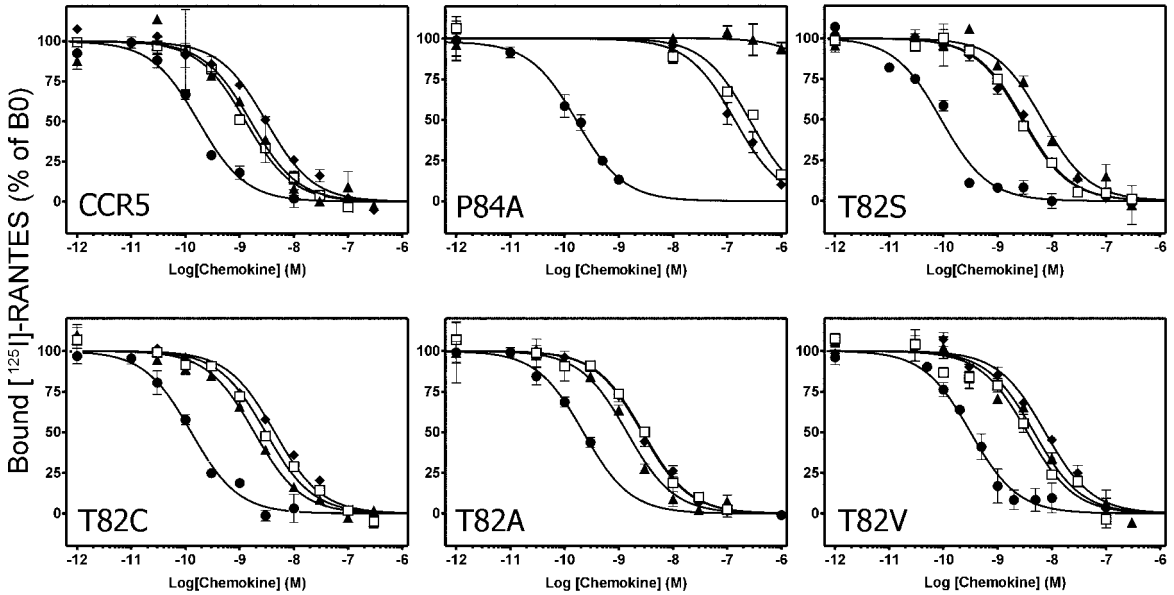

FIG. 4. **Binding properties of the WT and mutant receptors.** Competition binding assays were performed on CHO-K1 cell lines expressing WT CCR5 and the different mutants using ^{125}I-RANTES as tracer. The data are representative of at least two experiments. Results were analyzed by the GraphPad Prism software, using a single-site model, and the data were normalized for nonspecific (0%) and specific binding in the absence of competitor (100%). All points were run in triplicate (*error bars* represent S.E.). Unlabeled ligands are as follows: RANTES (●), MIP-1β (□), MIP-1α (▲), and MCP2 (♦).

TABLE III
Binding and functional properties of WT CCR5 and mutant receptors

The pIC_{50} (-log *M*) values were obtained from competition binding experiments, using ^{125}I-RANTES as a tracer (as displayed in Fig. 4). Values represent the mean ± S.E. of at least two independent determinations. The pEC_{50} (-log *M*) values were obtained from functional dose-response curves using the aequorin assay (as displayed in Fig. 5). Values represent the mean ± S.E. of at least three independent determinations.

	RANTES		MIP-1β		MIP-1α		MCP-2	
	pIC_{50}	pEC_{50}	pIC_{50}	pEC_{50}	pIC_{50}	pEC_{50}	pIC_{50}	pEC_{50}
CCR5	9.61 ± 0.14	8.48 ± 0.07	8.88 ± 0.01	8.15 ± 0.03	8.52 ± 0.23	7.62 ± 0.09	8.65 ± 0.11	7.70 ± 0.19
P84A	9.73 ± 0.03	7.82 ± 0.02	6.61 ± 0.03	<6	<6	<6	6.92 ± 0.02	<6
T82S	9.79 ± 0.13	8.36 ± 0.06	8.71 ± 0.16	7.54 ± 0.09	8.31 ± 0.14	7.43 ± 0.11	8.54 ± 0.01	7.47 ± 0.12
T82C	9.61 ± 0.20	8.14 ± 0.06	8.49 ± 0.03	7.38 ± 0.14	8.84 ± 0.11	7.83 ± 0.09	8.37 ± 0.05	<6
T82A	9.56 ± 0.09	8.22 ± 0.06	8.52 ± 0.03	7.22 ± 0.04	8.81 ± 0.04	7.36 ± 0.18	8.36 ± 0.22	6.84 ± 0.06
T82V	9.55 ± 0.10	7.76 ± 0.08	8.44 ± 0.01	6.36 ± 0.06	8.64 ± 0.31	6.87 ± 0.03	8.25 ± 0.06	<6

binding, with IC_{50} values right-shifted by 3 orders of magnitude (Fig. 4 and Table III). MIP-1α does not compete for the bound tracer, even at the highest concentration tested (1 μM).

RANTES displays an unaffected affinity for the CCR5 mutants T82S, T82C, T82A, and T82V, with IC_{50} values ranging from 0.2 to 0.3 nM. The three other ligands show affinities that are about 10 times lower than RANTES for all Thr-82 mutants, as already observed for WT CCR5. MIP-1β, MIP-1α, and MCP-2 display roughly WT affinities for all four Thr-82 mutants, with only mild variations according to the mutant. Their IC_{50} values are all in the range of 1.5–5.7 nM, confirming that none of the Thr-82 mutants have significantly affected binding properties. The largest change is a 3-fold increase in average IC_{50} for MIP-1β binding to T82V.

In summary, we find that all of the analyzed mutants bind the agonists RANTES, MIP-1α, MIP-1β, and MCP-2 with WT affinities. One exception is the P84A mutant. Although it binds RANTES as well as the WT receptor, its affinity for MIP-1β and MCP-2 is reduced, and it does not bind MIP-1α.

Functional Activation of the Mutants by CCR5 Agonists—A third and crucial set of tests was performed in order to investigate the ability of the five CCR5 mutants to be activated by the same four agonists. This was done using a sensitive assay based on the use of apoaequorin as a reporter system for intracellular calcium release. Activation of chemokine receptors, including CCR5, is known to result in calcium signaling. Control stimulation of the cell lines was achieved with a saturating concentration of ATP, which activates endogenously expressed P_2Y_2 receptors and generates a strong luminescent signal. We measured the cell response to ATP in all experiments and normalized the results as a percentage of this signal.

Fig. 5 shows typical activation curves obtained for the six WT and mutant receptors using the four agonists. In agreement with previous observations (4), we find that RANTES is the most potent agonist of WT CCR5, with an EC_{50} of 3.5 nM (Table III), whereas the EC_{50} of MIP-1β is twice as large on average (7.2 nM), and MCP-2 and MIP-1α are somewhat less efficient with average EC_{50} values of 23.4 and 25.0 nM, respectively.

However, unlike for the binding assays, in which all mutants except P84A displayed a WT-like binding behavior, the functional assay demonstrated various degrees of impairment for the different mutants. The CCR5 mutants with the most impaired function are P84A and T82V. P84A is activated by RANTES, with an average EC_{50} right-shifted by about 1 order of magnitude (one log unit in Fig. 5) and an E_{max} reaching only 20% of the ATP signal. But strikingly, none of the other three agonists elicits any detectable signal in this functional assay. This is not too surprising for MIP-1α, considering its severely decreased affinity for this mutant (IC_{50} >1000 nM). MIP-1β and MCP-2, however, did not activate P84A, even at 300 nM (MCP-2) or 1000 nM (MIP-1β) concentrations (data not shown), despite full ^{125}I-RANTES displacement at these concentrations in the binding assay.

The strongly reduced functional response of the T82V mu-

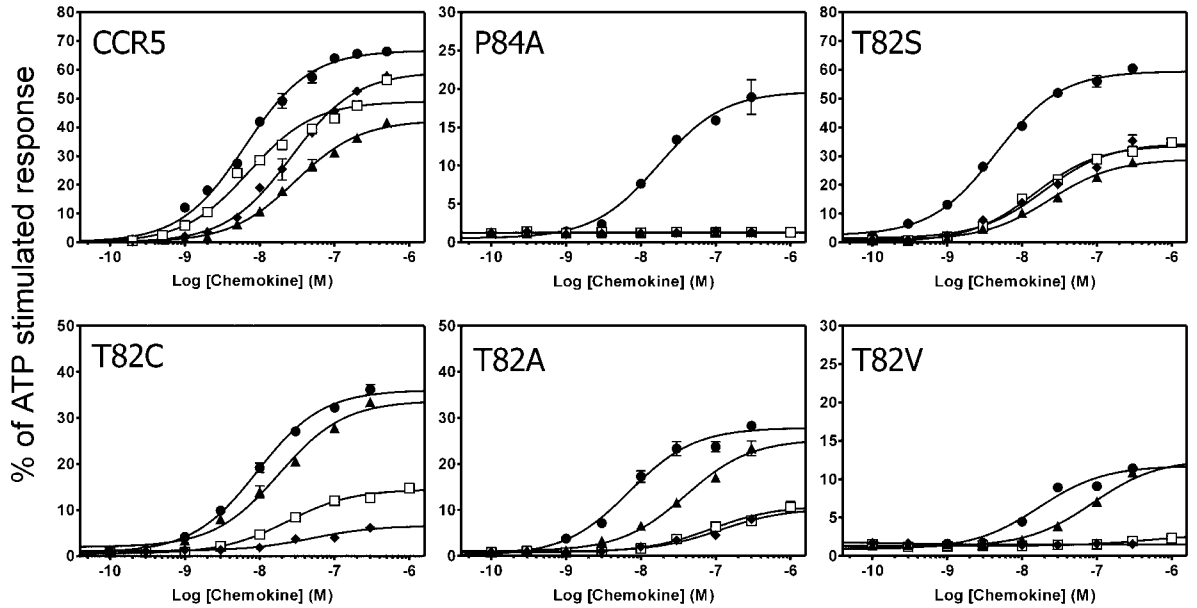

FIG. 5. **Activation of the different receptors by the four CCR5 agonists.** Shown is the functional response to RANTES (●), MIP-1β (□), MIP-1α (▲), and MCP-2 (♦) of CHO-K1 cells expressing WT CCR5 or the various mutants using the aequorin assay. All points were run in triplicate (*error bars* represent S.E.). The displayed curves represent a typical experiment out of at least three performed independently. Results were analyzed by nonlinear regression using the GraphPad Prism software. Data were normalized to maximal cell line stimulation by a saturating concentration of ATP. Note that the *vertical scales* of the *graphs* have been adapted to the maximal responses obtained for each line.

tant is somewhat surprising, especially in light of the milder functional impairment observed for T82A (Fig. 5). Indeed, the substitution of Thr by Val is isosteric. It preserves the β-branched character of the side chain and hence presents a less drastic change than a substitution by Ala, which truncates the side chain beyond the C_β atom. T82V displays a dramatically reduced response to RANTES, with the activation curve for this ligand shifted to the right by more than 1 order of magnitude. With MIP-1α, high concentrations are required (EC_{50} = 136 nM) to achieve moderate signals, whereas MIP-1β is unable to elicit detectable signals from this mutant in most experiments, although in some cases, a very weak response is measured at the highest concentrations. MCP-2 induces no response in T82V, although a normal binding affinity is measured for this chemokine, as shown above.

The T82A mutant comes next in the degree of functional impairment. RANTES remains the best agonist for this mutant, followed by MIP-1α (EC_{50} = 52 nM), and both ligands display a reduced E_{max} (~30% of maximum response). MIP-1β stimulates T82A with an EC_{50} of 63 nM and MCP-2 with an EC_{50} averaging 147 nM, both with a very low efficacy (E_{max} values below 15%; Fig. 5, Table III).

The mutants whose activities are least affected are T82S and T82C. T82S is stimulated by RANTES to a similar degree as WT CCR5, with an EC_{50} of 4.5 nM and an E_{max} of 60%. MIP-1β, MIP-1α, and MCP-2 show similar activation profiles with this mutant, characterized by a strong functional response, with an EC_{50} moderately displaced to the right and an E_{max} somewhat lower than for WT CCR5. RANTES and MIP-1α stimulate the T82C mutant with WT potencies but reduced E_{max}. MIP-1β elicits a poor response on this mutant, while MCP-2 is almost inactive.

These results taken together provide evidence on the important role played by Thr-82 and Pro-84 in CCR5 activation. The extent to which the activation of these mutants is affected by the series of agonists, measured under similar conditions, leads to the following ranking in terms of impairment of receptor activation: P84A > T82V > T82A > T82C > T82S.

DISCUSSION

In this study, we identified a sequence motif T*X*P, in TM2 of chemokine receptors, which is conserved throughout this important subfamily of GPCRs. We made the hypothesis that it plays an important role in receptor function and investigated this putative role by using a combination of theoretical and experimental techniques. Here, the findings from the two types of techniques are brought together and rationalized in light of our current knowledge of the CCR5 receptor structural and functional properties. This leads to the proposal of a mechanism for the implication of the T*X*P motif in CCR5 activation.

The TXP Motif Is a Structural Determinant in Chemokine Receptors—The molecular dynamics simulations, whose aim was to investigate how the side chain at position i-2 from the Pro residue affects the intrinsic conformational properties of a Pro-containing α-helix, lead to the following main conclusions: the presence of Thr, Ser, and Cys side chains at position i-2 increases the average PK angle by about 10°, whereas Val at that position has a negligible effect. The fact that the Val side chain is nonpolar and the observation that the other analyzed side chains, which were all polar, formed hydrogen bonds with the helix backbone during the simulations suggests that the observed effect on the bending angle arises from local deformations in helix geometry induced by these bonds.

Our modeling exercise, using the high resolution three-dimensional structure of rhodopsin, suggests that the presence of the T*X*P motif in TM2 would require a rearrangement of the TM helix bundle interactions in the chemokine receptors relative to rhodopsin.

In particular, Pro in position *2.58* would orient the extracellular part of TM2 toward TM3 and not close to TM1 as in rhodopsin; the addition of a Thr at i-2, as in the T*X*P motif, furthermore directs this part of TM2 toward the center of the bundle (Fig. 2, *C* and *D*). Our modeling study also suggests that in chemokine receptors, the extracellular region of TM2 would interact with TM3 and possibly with TM7, which is not feasible in the rhodopsin structure.

Our results thus lead us to suggest that the T*X*P motif in

TM2 is a structural determinant, in chemokine receptors, by virtue of significant local effects on the helix conformation, which propagate through a lever action to the extracellular parts of the TM bundle. It is noteworthy that there is ample experimental evidence that this region of GPCRs is involved in their functional properties (16), which suggests in turn that mutants modifying these local conformational effects should also modify receptor function.

Role of the TXP Motif in Ligand-induced Activation of CCR5—Our functional studies of T*X*P mutants of CCR5 were aimed at verifying this suggestion. The P84$^{2.58}$A mutant displayed a significantly affected pattern of binding for some ligands. We hypothesize that the profound structural perturbation in this mutant, caused by the abrogation of the PK, might change the conformation of some part of the extracellular domain, thus modifying the interactions with ligands. In agreement with this view, this putative conformational change could also be responsible for the observed decrease in recognition of the P84$^{2.58}$A mutant by monoclonal antibodies directed at conformational epitopes. This suggests that this PK is mandatory for the structural integrity of the protein. Alanine replacement of Pro-84$^{2.58}$ abolished the functional response of CCR5 to any of its agonists with the exception of RANTES, which induced minute activity, demonstrating the central role of this PK in the activation process.

All tested chemokines bound the various Thr-82$^{2.56}$ mutants with unchanged affinity, indicating that this residue is not involved in direct interaction with the ligands. In contrast to the binding properties, the chemokine-induced activation of CCR5 was quite sensitive to mutations of Thr-82$^{2.56}$, showing a gradation of the effects corresponding to that observed in the simulation.

Activation profiles of T82$^{2.56}$S showed mild differences with those of WT CCR5. However, this mutant had a reduced $E_{max,}$ when stimulated with MIP-1α, MIP-1β, and MCP-2. This behavior is reminiscent of that observed with partial agonists on WT receptors and hence suggests that these chemokines cannot fully activate this mutant.

This could occur if the equilibrium between the active and inactive forms of T82$^{2.56}$S is somewhat shifted toward the inactive one. The fact that RANTES activates this mutant normally could mean that it stabilizes more efficiently the active forms. The results of our MD simulations on the SAP-containing peptide suggest a molecular explanation to this shift in equilibrium. They show that this peptide features a similar α-helix kink geometry as in the TAP-containing peptide when Ser is in the $g+$ conformation but adopts a very different orientation of the PK when this side chain is in $g-$ (see Fig. 2*B*). This latter conformation may stabilize the inactive form of mutant receptors. This effect of Ser might possibly also explain the paucity of Ser residues at position 2.56 in the chemokine receptors (only 4 of 55 members have it).

The isosteric mutant T82$^{2.56}$V was even more impaired in the functional tests than T82$^{2.56}$A. T82$^{2.56}$V required high chemokine concentrations to trigger very modest activities, although the binding properties were not significantly affected for any of the ligands tested. We cannot provide a simple explanation for the difference of phenotype observed between these two mutants, but considering the observations made in the MD simulations, the hydrogen bonding capacity of the side chain at position *2.56* seems to be a more important feature for activation than the β-branched character of the side chain.

Our results show that, in chemokine receptors, the Pro in TM2 is crucial for proper receptor activation and that the conserved Thr located 2 positions before the Pro modulates the function of the receptor. The experiments therefore confirm the theoretical hypothesis stating that the T*X*P motif plays a key structural role in chemokine receptors, the PK constituting the main element and the Thr acting as a modulator of this PK. Moreover, this motif is mainly involved in receptor activation but plays little role in ligand binding. These results also demonstrate that high affinity binding of chemokines by CCR5 is not dependent on the coupling state with G-proteins. A previous description of other non-functional CCR5 mutants characterized by unimpaired affinities for their chemokine ligands (10) supports this hypothesis. Along the same line of evidence, it is well established that NH_2-terminally truncated chemokines often keep their high affinities for their cognate receptors while becoming antagonists or weak partial agonists.

New Insights into Chemokine-induced Activation—Surprisingly, although the T*X*P motif is present in all chemokine receptors, functional alteration observed in the Thr-82$^{2.56}$ mutants is strongly chemokine-dependent. RANTES is the least affected agonist, MCP-2 being strongly sensitive to all mutations, while MIP-1α and MIP-1β behave as partial agonists for the various mutants. How can we explain these observations?

Interestingly, RANTES differs structurally from the other CCR5 agonists in its amino terminus, with 9 residues before the first conserved cysteine for RANTES and 10 residues for the three other ligands. Also, the sequence of the MCP-2 NH_2 terminus is somewhat different from that of the other agonists, whereas those of MIP-1α and MIP-1β are quite similar to each other. Hence, there seems to be a relation between the sensitivity of receptor activation by the different chemokines to the mutations in T*X*P and the differences between the NH_2-terminal regions of these molecules. It is significant that these regions were shown to be important in receptor activation by mutation and deletion experiments (6, 7).

This leads us to formulate the hypothesis that chemokine induced activation involves interactions of the ligand NH_2 terminus with the portion of transmembrane domain whose conformation may be modulated by the T*X*P motif. Thus, the differences in behavior among ligands could result from differences in these interactions. This hypothesis could be investigated by testing mutant receptor activation by chimeric chemokines exchanging the NH_2 terminus or the core region.

As mentioned above, chemokines truncated in their NH_2 terminus often still elicit some functional responses at high concentrations and hence behave as partial agonists. This parallels the effects of full-size chemokines on our Thr-82$^{2.56}$ mutant series and could result from the binding of the chemokine core region to the extracellular loops of the receptor. It was proposed that this interaction would induce partial signal transduction, characterized by inhibition of cAMP, but would not trigger calcium influx or chemotaxis (6). Thus, it does not contradict our proposal that full activation involves interactions with the NH_2-terminal region of the chemokine.

Based on chimeras between CCR2b and CCR1, it was recently proposed that activation of chemokine receptors involves the first extracellular loop ECL1 (53). Having shown here that TM2 in this receptor family extends to position *2.67*, the effects of these chimeras are most probably due to the exchange of variable residues at the extracellular portion of this helix, rather than to the swap of ECL1, which is well conserved in these receptors. Interestingly, these changes produced mutant receptors with good ligand affinity but impaired chemokine-induced functional response. These data parallel our present finding and hence agree with our hypothesis on the importance of the extracellular part of TM2 in receptor activation.

Other recent studies have described low molecular weight chemical compounds acting as antagonists (54–56) with promising applications in inflammatory diseases and HIV infection.

Interestingly, the binding sites of these antagonists have been located within the transmembrane bundle of the receptors (57, 58). Insights provided here on the role of structural determinants in this region may therefore be helpful in further elucidating the action of these compounds and in designing effective drugs. The availability of the high resolution structure of rhodopsin will greatly facilitate this task and allow more detailed analyses of the type described here to be extended to other rhodopsin-like GPCRs.

Acknowledgments—Expert technical assistance was provided by M. J. Simons, and Jean Richelle is gratefully acknowledged for valuable help with the computer systems. We thank Mathias Mack for kindly providing monoclonal antibodies and Harel Weinstein for helpful discussions.

REFERENCES

1. Baggiolini, M. (1998) *Nature* **392,** 565–568
2. Littman, D. R. (1998) *Cell* **93,** 677–680
3. Samson, M., Libert, F., Doranz, B. J., Rucker, J., Liesnard, C., Farber, C. M., Saragosti, S., Lapoumeroulie, C., Cognaux, J., Forceille, C., Muyldermans, G., Verhofstede, C., Burtonboy, G., Georges, M., Imai, T., Rana, S., Yi, Y., Smyth, R. J., Collman, R. G., Doms, R. W., Vassart, G., and Parmentier, M. (1996) *Nature* **382,** 722–725
4. Blanpain, C., Migeotte, I., Lee, B., Vakili, J., Doranz, B. J., Govaerts, C., Vassart, G., Doms, R. W., and Parmentier, M. (1999) *Blood* **94,** 1899–1905
5. Hemmerich, S., Paavola, C., Bloom, A., Bhakta, S., Freedman, R., Grunberger, D., Krstenansky, J., Lee, S., McCarley, D., Mulkins, M., Wong, B., Pease, J., Mizoue, L., Mirzadegan, T., Polsky, I., Thompson, K., Handel, T. M., and Jarnagin, K. (1999) *Biochemistry* **38,** 13013–13025
6. Jarnagin, K., Grunberger, D., Mulkins, M., Wong, B., Hemmerich, S., Paavola, C., Bloom, A., Bhakta, S., Diehl, F., Freedman, R., McCarley, D., Polsky, I., Ping-Tsou, A., Kosaka, A., and Handel, T. M. (1999) *Biochemistry* **38,** 16167–16177
7. Gong, J. H., and Clark-Lewis, I. (1995) *J. Exp. Med.* **181,** 631–640
8. LaRosa, G. J., Thomas, K. M., Kaufmann, M. E., Mark, R., White, M., Taylor, L., Gray, G., Witt, D., and Navarro, J. (1992) *J. Biol. Chem.* **267,** 25402–25406
9. Ahuja, S. K., and Murphy, P. M. (1996) *J. Biol. Chem.* **271,** 20545–20550
10. Farzan, M., Choe, H., Martin, K. A., Sun, Y., Sidelko, M., Mackay, C. R., Gerard, N. P., Sodroski, J., and Gerard, C. (1997) *J. Biol. Chem.* **272,** 6854–6857
11. Blanpain, C., Doranz, B. J., Vakili, J., Rucker, J., Govaerts, C., Baik, S. S., Lorthioir, O., Migeotte, I., Libert, F., Baleux, F., Vassart, G., Doms, R. W., and Parmentier, M. (1999) *J. Biol. Chem.* **274,** 34719–34727
12. Samson, M., LaRosa, G., Libert, F., Paindavoine, P., Detheux, M., Vassart, G., and Parmentier, M. (1997) *J. Biol. Chem.* **272,** 24934–24941
13. Palczewski, K., Kumasaka, T., Hori, T., Behnke, C. A., Motoshima, H., Fox, B. A., Le, T., I, Teller, D. C., Okada, T., Stenkamp, R. E., Yamamoto, M., and Miyano, M. (2000) *Science* **289,** 739–745
14. Unger, V. M., Hargrave, P. A., Baldwin, J. M., and Schertler, G. F. (1997) *Nature* **389,** 203–206
15. Strader, C. D., Fong, T. M., Graziano, M. P., and Tota, M. R. (1995) *FASEB. J.* **9,** 745–754
16. Ji, T. H., Grossmann, M., and Ji, I. (1998) *J. Biol. Chem.* **273,** 17299–17302
17. Gether, U., and Kobilka, B. K. (1998) *J. Biol. Chem.* **273,** 17979–17982
18. Elling, C. E., Nielsen, S. M., and Schwartz, T. W. (1995) *Nature* **374,** 74–77
19. Sheikh, S. P., Vilardarga, J. P., Baranski, T. J., Lichtarge, O., Iiri, T., Meng, E. C., Nissenson, R. A., and Bourne, H. R. (1999) *J. Biol. Chem.* **274,** 17033–17041
20. Sheikh, S. P., Zvyaga, T. A., Lichtarge, O., Sakmar, T. P., and Bourne, H. R. (1996) *Nature* **383,** 347–350
21. Farrens, D. L., Altenbach, C., Yang, K., Hubbell, W. L., and Khorana, H. G. (1996) *Science* **274,** 768–770
22. Dunham, T. D., and Farrens, D. L. (1999) *J. Biol. Chem.* **274,** 1683–1690
23. Javitch, J. A., Fu, D., Liapakis, G., and Chen, J. (1997) *J. Biol. Chem.* **272,** 18546–18549
24. Rasmussen, S. G., Jensen, A. D., Liapakis, G., Ghanouni, P., Javitch, J. A., and Gether, U. (1999) *Mol. Pharmacol.* **56,** 175–184
25. Gether, U., Lin, S., Ghanouni, P., Ballesteros, J. A., Weinstein, H., and Kobilka, B. K. (1997) *EMBO J.* **16,** 6737–6747
26. Barlow, D. J., and Thornton, J. M. (1988) *J. Mol. Biol.* **201,** 601–619
27. Woolfson, D. N., and Williams, D. H. (1990) *FEBS Lett.* **277,** 185–188
28. Ballesteros, J. A., and Weinstein, H. (1995) *Methods Neurosci.* **25,** 366–428
29. Kolakowski, L. F., Jr., Lu, B., Gerard, C., and Gerard, N. P. (1995) *J. Biol. Chem.* **270,** 18077–18082
30. Nakayama, T. A., and Khorana, H. G. (1991) *J. Biol. Chem.* **266,** 4269–4275
31. Tonacchera, M., Chiovato, L., Pinchera, A., Agretti, P., Fiore, E., Cetani, F., Rocchi, R., Viacava, P., Miccoli, P., and Vitti, P. (1998) *J. Clin. Endocrinol. Metab.* **83,** 492–498
32. Javitch, J. A., Fu, D., and Chen, J. (1995) *Biochemistry* **34,** 16433–16439
33. Wess, J., Nanavati, S., Vogel, Z., and Maggio, R. (1993) *EMBO J.* **12,** 331–338
34. Hong, S., Ryu, K. S., Oh, M. S., Ji, I., and Ji, T. H. (1997) *J. Biol. Chem.* **272,** 4166–4171
35. Vichi, P., Whelchel, A., and Posada, J. (1999) *J. Biol. Chem.* **274,** 10331–10338
36. Barak, L. S., Menard, L., Ferguson, S. S., Colapietro, A. M., and Caron, M. G. (1995) *Biochemistry* **34,** 15407–15414
37. Blundell, T., Barlow, D., Borkakoti, N., and Thornton, J. (1983) *Nature* **306,** 281–283
38. Ballesteros, J., Deupi, X., Olivella, M., Haaksma, E., and Pardo, L. (2000) *Biophys. J.* **79,** 2754–2760
39. Ri, Y., Ballesteros, J. A., Abrams, C. K., Oh, S., Verselis, V. K., Weinstein, H., and Bargiello, T. A. (1999) *Biophys. J.* **76,** 2887–2898
40. Wintjens, R. T., Rooman, M. J., and Wodak, S. J. (1996) *J. Mol. Biol.* **255,** 235–253
41. Gray, T. M., and Matthews, B. W. (1984) *J. Mol. Biol.* **175,** 75–81
42. McGregor, M. J., Islam, S. A., and Sternberg, M. J. (1987) *J. Mol. Biol.* **198,** 295–310
43. Darden, T., York, D., and Pedersen, L. (1993) *J. Chem. Phys.* **98,** 10089–10092
44. Case, D. A., Pearlman, D. A., Caldwell, J. W., Cheatham, T. E., Ross, W. S., Simmerling, C. L., Darden, T. A., Merz, K. M., Stanton, R. V., Cheng, A. L., Vincent, J., Crowley, M., Ferguson, D. M., Radmer, R. J., Seibel, G. L., Singh, U. C., Weiner, P. K., and Kollman, P. A. (1997) *AMBER5*, University of California, San Francisco
45. Cornell, W. D., Cieplak, P., Bayly, C. I., Gould, I. R., Merz, K. M., Jr., F., D. M. Spellmeyer, D. C., Fox, T., Caldwell, J. W., and Kollman, P. A. (1995) *J. Am. Chem. Soc.* **117,** 5179–5197
46. Kelley, L. A., Gardner, S. P., and Sutcliffe, M. J. (1996) *Protein Eng.* **9,** 1063–1065
47. Rizzuto, R., Pinton, P., Carrington, W., Fay, F. S., Fogarty, K. E., Lifshitz, L. M., Tuft, R. A., and Pozzan, T. (1998) *Science* **280,** 1763–1766
48. Stables, J., Green, A., Marshall, F., Fraser, N., Knight, E., Sautel, M., Milligan, G., Lee, M., and Rees, S. (1997) *Anal. Biochem.* **252,** 115–126
49. Blanpain, C., Lee, B., Vakili, J., Doranz, B. J., Govaerts, C., Migeotte, I., Sharron, M., Dupriez, V., Vassart, G., Doms, R. W., and Parmentier, M. (1999) *J. Biol. Chem.* **274,** 18902–18908
50. Horn, F., Weare, J., Beukers, M. W., Horsch, S., Bairoch, A., Chen, W., Edvardsen, O., Campagne, F., and Vriend, G. (1998) *Nucleic Acids Res.* **26,** 275–279
51. Yun, R. H., Anderson, A., and Hermans, J. (1991) *Proteins* **10,** 219–228
52. Javitch, J. A., Ballesteros, J. A., Weinstein, H., and Chen, J. (1998) *Biochemistry* **37,** 998–1006
53. Han, K. H., Green, S. R., Tangirala, R. K., Tanaka, S., and Quehenberger, O. (1999) *J. Biol. Chem.* **274,** 32055–32062
54. Donzella, G. A., Schols, D., Lin, S. W., Este, J. A., Nagashima, K. A., Maddon, P. J., Allaway, G. P., Sakmar, T. P., Henson, G., De Clercq, E., and Moore, J. P. (1998) *Nat. Med.* **4,** 72–77
55. Baba, M., Nishimura, O., Kanzaki, N., Okamoto, M., Sawada, H., Iizawa, Y., Shiraishi, M., Aramaki, Y., Okonogi, K., Ogawa, Y., Meguro, K., and Fujino, M. (1999) *Proc. Natl. Acad. Sci. U. S. A.* **96,** 5698–5703
56. Hesselgesser, J., Ng, H. P., Liang, M., Zheng, W., May, K., Bauman, J. G., Monahan, S., Islam, I., Wei, G. P., Ghannam, A., Taub, D. D., Rosser, M., Snider, R. M., Morrissey, M. M., Perez, H. D., and Horuk, R. (1998) *J. Biol. Chem.* **273,** 15687–15692
57. Dragic, T., Trkola, A., Thompson, D. A., Cormier, E. G., Kajumo, F. A., Maxwell, E., Lin, S. W., Ying, W., Smith, S. O., Sakmar, T. P., and Moore, J. P. (2000) *Proc. Natl. Acad. Sci. U. S. A.* **97,** 5639–5644
58. Mirzadegan, T., Diehl, F., Ebi, B., Bhakta, S., Polsky, I., McCarley, D., Mulkins, M., Weatherhead, G. S., Lapierre, J. M., Dankwardt, J., Morgans, D., Jr., Wilhelm, R., and Jarnagin, K. (2000) *J. Biol. Chem.* **275,** 25562–25571
59. Javitch, J. A., Ballesteros, J. A., Chen, J., Chiappa, V., and Simpson, M. M. (1999) *Biochemistry* **38,** 7961–7968